UCRL-17043

University of California

Ernest O. Lawrence Radiation Laboratory

NATURAL CONVECTION COOLANT FOLLOWING LOSS-OF-COOLANT

Berkeley, California

DISCLAIMER

Submitted To:
Nuclear Science and Engineering

UCRL-17043

UNIVERSITY OF CALIFORNIA
Lawrence Radiation Laboratory
Berkeley, California

AEC Contract No. W-7405-eng-48

NATURAL CONVECTION COOLING FOLLOWING LOSS-OF-COOLANT

R. P. Omberg, D. R. Olander, and V. E. Schrock

August 1966

NATURAL CONVECTION COOLING FOLLOWING LOSS-OF-COOLANT

R. P. Omberg, D. R. Olander, and V. E. Schrock

Inorganic Materials Research Division, Lawrence Radiation Laboratory,
and Department of Nuclear Engineering,
University of California, Berkeley, California

August 1966

ABSTRACT

The effect of natural convection upon the temperature transient following a loss-of-coolant accident was analized for a simplified power reactor configuration. The analysis was based on the one-dimensional quasi-steady state form of the flow conservation equations coupled to a lumped capacity transient energy fuel equation. The natural convection process was taken as the only mode of heat removal. A constant radial power density was assumed, the time dependence of the decay heat was considered, and the heat transfer and frictional losses assumed to be characteristic of turbulent pipe flow. The system of equations developed was solved using the design parameters for the Loss-of-Fluid Test Reactor (LOFT). It was found that natural convection is an important mechanism for heat removal in loss-of-coolant analyses for reactors of the LOFT type. Clad melting was prevented for operating power levels less than about 70% of rated power (50 Mw for the LOFT). In addition, if simultaneous rupture of the external piping to and from the pressure vessel were to occur, the analysis predicts a maximum temperature less than the melting temperature of the cladding.

I. INTRODUCTION

Most calculations of the temperature transient following a loss-of-coolant accident in a nuclear power reactor neglect the effect of natural convection. A study of the hazards analyses for several operating power reactors indicated that while heat transfer by conduction and thermal radiation were considered, heat removal due to natural convection was neglected in each case.[1-6] In the case of the Loss-of-Fluid Test Reactor (LOFT), Jensen, et al. considered natural convection; however, as the conduction and radiation mechanisms were emphasized, the treatment of natural convection was simplified.[7] If conduction and thermal radiation are neglected and the natural convection process considered to act alone, a treatment considerably more detailed than that of Ref. 7 is possible. For this case, Olander, et al. have shown that in a low power reactor of the TRIGA type, cooling by natural convection prevents core damage after an excursion.[8] The analysis presented here is similar to that of Ref. 8, but in addition considers temperature dependent coolant properties and employs a simplified power reactor configuration. As in Ref. 8 natural convection is considered to be the sole mode of heat removal. The specific assumptions are

1. The power density is constant radially and varies as a full cosine axially and the time dependence of the heat decay is given by Ref. 9. The operating time prior to shutdown is assumed infinite; the blowdown is assumed to occur instantly and to completely empty the core and external piping of liquid.
2. The flow through the system can be described by the quasi-steady state form of the one-dimensional conservation equations with frictional losses and heat transfer characteristic

of turbulent pipe flow.

3. The flow equations are coupled to the lumped capacity transient energy equation for small axial sections of fuel, which neglects axial conduction and assumes radially uniform temperature in the rod.

The reactor configuration employed is shown in Fig. 1; the reactor core is located in the lower half of the pressure vessel and an equivalent length of pipe represents the external piping and fittings. The break is assumed to take place at the upper junction of the piping with the pressure vessel. Steam from the containment vessel then enters and passes through the piping with no temperature increase until reaching the core. After rising through the core, the coolant flows upward through the region above the core (denoted as the stack) at constant temperature with no wall friction. The system was further idealized by assuming that all valves, including check valves, are completely open and the system to contain only water vapor after blowdown. The temperature of the entering coolant is assumed constant during the transient.

II. CALCULATION METHOD

The one-dimensional flow equations governing conservation of mass, momentum, and energy in the coolant are:

$$\frac{\partial \rho}{\partial t} + \frac{\partial}{\partial x}(\rho u) = 0 \qquad (1)$$

$$\frac{\partial}{\partial t}(\rho u) + \frac{\partial}{\partial x}(\rho u^2) = -\frac{\partial p}{\partial x} - \rho g - \frac{f}{2}\frac{\rho u^2}{r_H} \qquad (2)$$

$$\frac{\partial}{\partial t}\left(\rho\left(E + \frac{u^2}{2}\right)\right) + \frac{\partial}{\partial x}\left(\rho u\left(H + \frac{u^2}{2}\right)\right) = \frac{q_w}{r_H'} - \rho u g \quad (3)$$

The energy equation in the fuel is, in accordance with assumption (3):

$$(\rho c_p)_f \frac{\partial T_f}{\partial t} = Q(t) \sin(\pi x/L) - \frac{A_T}{A_f r_H} q_w \quad (4)$$

Defining $G = \rho u$, neglecting potential and kinetic energy in Eq. (3), and imposing the quasi-static approximation, the coolant equations reduce to a coupled set of ordinary differential equations:

$$\frac{dG}{dx}(x,t) = 0 \quad (5)$$

$$\frac{dp}{dx} = -\frac{d}{dx}\left(\frac{G^2}{\rho}\right) - \rho g - \frac{fG^2}{2\rho r_H} \quad (6)$$

$$\frac{d}{dx}(GH) = \frac{q_w}{r_H'} \quad (7)$$

$$\frac{dT_f}{dt} = \frac{Q(t)\sin(\pi x/L)}{(\rho c_p)_f} \frac{A_F}{(\rho c_p)_f r_H A_f} q_w \quad (8)$$

The effect of these approximations will be evaluated later. Using the ideal gas law and neglecting the slight pressure drop through the core, the density is:

$$\rho = \rho_1 T_1 / T \quad (9)$$

The viscosity variation with temperature is assumed as:

$$\mu = \mu_1 (T/T_1)^{\ell} \quad (10)$$

and the friction factor is assumed given by:

$$f = K\ Re^{-n} \tag{11}$$

where for turbulent pipe flow K = 0.046 and n = 0.2. With the wall heat flux taken as $q_w = h(T_f - T)$ and $dH = c_p\, dT$, Eqs. (5) - (8) become:

$$\frac{d}{d\xi}\ (\theta^{\ell}\ Re) = 0 \tag{12}$$

$$\frac{dP}{d\xi} = \frac{1}{c}\ Re^2(0,t)\ \frac{d\theta}{d\xi} - \frac{KL}{2r_H c}\ \frac{Re^2(0,t)}{Re^n\ (x,t)} - \frac{1}{\theta} \tag{13}$$

$$\frac{d\theta}{d\xi} + \frac{L}{r_H'}\ \frac{Nu\ (\xi,\tau)}{Pr \cdot Re(\xi,\tau)}\ \theta(\xi,\tau) = \frac{L}{r_H'}\ \frac{Nu\ (\xi,\tau)}{Pr \cdot Re\ (\xi,\tau)}\ \theta_f(\xi,\tau) \tag{14}$$

$$\frac{d\theta_f}{dt} + Nu\ (\xi,\tau)\ \theta_f(\xi,\tau) = \tilde{Q}(\tau)\ \sin\ (\pi\xi) + Nu\ (\xi,\tau)\ \theta(\xi,\tau) \tag{15}$$

with the following dimensionless variables and parameters:

$$\left.\begin{aligned}
\xi &= x/L \\
\tau &= \left(\frac{k_l(A_F/A_f)}{4\ r_H\ r_H'\ (\rho c_p)_f}\right) t \\
\theta &= T/T_l \\
\theta_f &= T_f/T_l \\
\delta &= L_{eq}/L \\
R &= L'/L \\
\tilde{Q} &= \left(\frac{4\ r_H\ r_H'}{k_l\ T_l\ (A_F/A_f)}\right) Q \\
P &= p/\rho_l\ g\ L \\
c &= 16\ r_H^2\ \rho_l g L/\mu_l^2
\end{aligned}\right\} \tag{16}$$

The boundary and initial conditions are

$$\begin{aligned} \mathrm{Re}\,(\xi,0) &= 0 \\ P(-\delta) &= P(R) \\ \theta(0,\tau) &= 1 \\ \theta_f(\xi,0) &= \text{constant} \end{aligned} \tag{17}$$

Integrating Eqs. (12-15) directly gives:

$$\mathrm{Re}\,(\xi,\tau) = \frac{\mathrm{Re}\,(0,\tau)}{\theta^{\ell}(\xi,\tau)} \tag{18}$$

$$\frac{C}{\mathrm{Re}^2(0,\tau)} \left\{ \int_0^1 \frac{1-\theta(\xi,\tau)}{\theta(\xi,\tau)}\, d\xi + \frac{1-\theta(1,\tau)}{\theta(1,\tau)} (R-1) \right\} +$$

$$[\theta(1,\tau) - 1] + \frac{KL}{2\, r_H} \left(\frac{1}{\mathrm{Re}^{n}(0,\tau)} \right) \int_0^1 (\theta^{1+n\ell}(\xi,\tau) + \delta)\, d\xi = 0 \tag{19}$$

$$\theta(\xi,\tau) = \left\{ \theta(0,\tau) + \frac{L}{r_H'} \int_0^{\xi} \theta_f(\xi',\tau)\, \frac{\mathrm{Nu}\,(\xi';\tau)}{\mathrm{Pr}\cdot\mathrm{Re}\,(\xi';\tau)} \right.$$

$$\left. \exp\left[\frac{L}{r_H'} \int_0^{\xi'} \frac{\mathrm{Nu}\,(\xi'';\tau)}{\mathrm{Pr}\cdot\mathrm{Re}(\xi'';\tau)}\, d\xi'' \right] d\xi' \right\} \tag{20}$$

$$\left[\exp\left(- \frac{L}{r_H'} \int_0^{\xi} \frac{\mathrm{Nu}\,(\xi';\tau)}{\mathrm{Pr}\cdot\mathrm{Re}\,(\xi';\tau)}\, d\xi' \right) \right]$$

$$\theta_f(\xi,\tau) = \left\{ \theta_f(\xi,0) + \int_0^{\tau} [\tilde{Q}(\tau')\, \sin(\pi\xi) + \right.$$

$$\left. \theta(\xi,\tau')\, \mathrm{Nu}\,(\xi,\tau')] \exp\left(\int_0^{\tau'} \mathrm{Nu}\,(\xi,\tau'')\, d\tau'' \right) d\tau' \right\} \tag{21}$$

$$\left[\exp\left(- \int_0^{\tau} \mathrm{Nu}\,(\xi,\tau')\, d\tau' \right) \right]$$

where the momentum equation has been integrated around the entire loop and Eqs. (18) and (20) integrated on $0 \leq \xi \leq 1$. A relation between the Nusselt Number and the Reynolds Number is now needed; the Dittus-Boelter relation was chosen for this:

$$Nu = 0.023\ Re^{0.8}\ Pr^{0.4} \qquad (22)$$

Forced convection relations for the friction factor and Nusselt Number should adequately describe the process since most of the buoyant force should be developed in the stack region above the core and hence the core should sense largely a forced convection process.

The set of Eqs (18-22) were solved numerically using an iterative technique described in Ref. 10. Briefly, this consists of putting an approximate solution into Eqs. (18-21), thus generating an improved approximation. This was continued until the maximum difference between successive iterations became smaller than a prescribed convergence criteria. The input parameters were based on those used in the design of the LOFT Reactor[7] since this reactor is intended to be parametrically typical of contemporary power reactors. The values used are shown in Table I.

III. RESULTS

The equations were solved for three midplane operating power densities: 61, 98, and 147 cal/cm^3-sec. A full cosine axial distribution was assumed, and with the constant radial power density assumption, the operating power can be obtained from the midplane density by the equation Power = $(2/\pi)\ Q\ A_f L$. The equivalent power levels are 31, 51, and 76 Mw, respectively.

The results are shown in Figs. 2-7. The maximum axial fuel temperature as a function of time is shown in Fig. 2. This axial maximum

TABLE I

Parameters Used in the Solution

Core	
Height, L (cm)	91
Hydraulic radius, r_H(cm)	0.48
Heated hydraulic radius, r_H' (cm)	0.496
Cross-sectional area for coolant, A_F(cm^2)	5130
Cross-sectional area of fuel, [a] A_f (cm^2)	2150
Equivalent length of external piping, [b] L_{eq}(cm)	400
Height of core plus stack region, L' (cm)	182
Fuel	
Density, [a] ρ_f(gm/cm^3)	9.45
Specific heat, [a] c_{pf} (cal/gm-°C)	0.115
Thermal conductivity, [a] k_f (cal/sec-cm-°C)	0.0242
Initial fuel temperature, T_{f_1} (independent of ξ)(°C)	260
Steam Coolant (at inlet)	
Pressure (psia)	35
Temperature, T_1 (°C)	127
Density, ρ_1 (gm/cm^3)	0.00135
Viscosity, μ_1 (poise)	0.000138
Thermal conductivity, k_1 (cal/sec-cm-°C)	$6.8 \cdot 10^{-5}$
Specific heat, C_{p_1} (cal/gm-°C)	0.52
Prandtl Number, Pr	1.05
Viscosity exponent, ℓ	0.98
$C = 16\, r_H^2\, \rho_1^2\, g\, L/\mu_1^2$	$3.14 \cdot 10^7$

a - These values are based on a homogenized mixture of fuel and cladding.(10)

b - The equivalent length was calculated from the flow conditions at steady-state operation.(10)

was located near the midplane position ($\xi \approx 0.5$) during the early part of the transient and, as time progressed, moved downstream to $\xi \approx 0.65$. The figure is a plot of this maximum temperature versus time independent of its position. It can be seen that the temperature passes through a temporal maximum and then decreases as a consequence of the decaying heat generation rate; at the maximum, all heat generated is being removed by natural convection. The radial temperature drop in a fuel element was calculated separately at the maximum temperature attained in Fig. 2 and was less than 25°C and hence insignificant. A comparison of these curves with the adiabatic case during the early part of the transient is shown in Fig. 3. It can be seen that the transient behaves very much like an adiabatic one for very short times while departing considerably from the adiabatic case for large times. If cladding and fuel melting temperatures of 1400 and 2800°C are assumed, then at 61 cal/cm^3-sec neither the cladding nor fuel will melt. At 98 cal/cm^3-sec, the time to reach the melting point of the cladding has been extended from the adiabatic value of 400 sec to 600 sec; the fuel melting point is not reached. At 147 cal/cm^3-sec, natural convection delays the onset of clad melting by 50 sec and fuel melting by 500 sec. In Fig. 4 the locus of the maxima from Fig. 2 are plotted giving the maximum fuel temperature (in time and position) as a function of operating power density. The power density at which the cladding melts is 70 cal/cm^3-sec or 36 Mw. If one presumes that the fuel maintains its integrity after the cladding has melted, the melting point of the fuel is attained for power densities of 126 cal/cm^3-sec or 65 Mw. A plot of the time to clad and fuel melting versus operating power density is shown in Fig. 5, with the adiabatic case shown for comparison. This figure shows that the effect of natural convection

cooling decreases with an increase in the power density and increases with an increase in the material melting point. There was some uncertainty in drawing the steam cooling curves due to the limited number of points and the approach to a vertical asymptote; thus the point at which melting did not occur is noted. Figure 6 shows the Reynolds Number as a function of time at the core inlet and exit. The Reynolds Number is slightly below the critical value of 2000 for smooth tubes at the inlet and significantly below it at the exit. This would at first seem to indicate the existence of laminar flow. However, the LOFT Reactor core departs significantly from a circular duct and has a flow distribution plate at the entrance which gives rise to an abrupt entrance effect. Investigations of abrupt entrances with decidedly non-circular ducts, in particular the work of Eckert and Irvine,[10,11] have shown the departure from the laminar regime to occur at Reynolds Numbers as low as 1000 with the turbulent regime fully established at 1800. Thus for a configuration such as a LOFT Reactor core, the flow is probably turbulent at the entrance. The core is approximately 48 hydraulic diameters long and has several spacer grids across the core perpendicular to the flow direction. Thus if turbulent flow exists at the inlet, the calming length probably exceeds the core length and turbulent flow should persist throughout the core.

An estimation of the magnitude of the change which would take place if laminar flow were to exist in all or part of the core can be made by assuming a laminar correlation for the friction factor and Nusselt Number. As an approximation, it was assumed the core could be represented by a circular pipe and the local Nusselt Number to be given by the asymptotic value of the constant wall heat flux case, i.e., 4.364. The results for

power density of 147 cal/cm^3-sec, the maximum previously considered, are shown in Fig. 7, where there is little difference in the fuel temperatures and the laminar Reynolds Number at the entrance quickly rises to a value higher than the corresponding turbulent case and above the critical value for smooth tubes. Thus after an initial acceleration period, the flow should be turbulent and the fact that laminar flow existed during this initial period should have little effect on the resulting fuel temperature for the cases considered. Also, this calculation indicates that if laminar flow were to exist near the core exit, the effect upon the resulting fuel temperatures should be negligible in these cases.

A calculation was also made to evaluate the effect of the external piping. If a double break is considered, the external piping will not enter into the circuit. The results for this case are shown in Fig. 8 for a power density of 147 cal/cm^3-sec. The Reynolds Numbers are considerably higher and the fuel temperatures considerably lower; the fuel reached 2500°C versus 3800°C previously. The fuel temperature transient with external piping from Fig. 2 is shown for comparison in Fig. 8.

The terms dropped in assuming the quasi-static form of the conservation equations were evaluated and with one exception found to be less than one percent of the terms retained for times greater than 25 seconds. The exception was that the axial conduction heat flux amounted to 5% of the wall heat flux.

IV. CONCLUSIONS

The calculations presented here were not intended to apply quantitatively to a particular reactor, but to demonstrate that natural convection is an important mechanism of heat removal in loss-of-coolant

analyses for reactors of the LOFT type. Buoyancy driven convective cooling prevents melting of the cladding for operating power levels less than about 70% of rated power (50 Mw for the LOFT). The computation is conservative in that heat removal by radiation and conduction have been neglected; it is optimistic in that the steam-metal reaction has been neglected, the power density was assumed independent of radial position, and the core and external piping were considered liquid-free at the beginning of the transient.

The analysis was based upon turbulent pipe flow formulas for frictional losses and heat transfer. This assumption appears to be adequate, since the computed Reynold's Numbers at the core inlet were between 1800 and 2000 for most of the transient and the complex geometry of the core structure probably inhibits the transition to laminar flow. In addition, a calculation based upon laminar flow friction and heat transfer produced little change in the time-temperature history of the fuel.

A calculation neglecting the frictional resistance of the external piping (which represents a simultaneous rupture of the piping to and from the pressure vessel) indicated that the maximum fuel temperature attained in the transient is considerably reduced; at a pre-shutdown power of 76 Mw, the fuel reached 3800°C (hypothetically) with the external piping in the circuit, and 2500°C without it. This suggests that it might be beneficial to devise a method which would open both the inlet and outlet piping connections to the pressure vessel in the event of a rupture anywhere in the loop. Such a method would simultaneously insure complete removal of liquid from the core and maximize the effectiveness of natural convection cooling of the core by steam from the containment vessel.

NOMENCLATURE

A_f	Cross-sectional area of fuel and cladding (cm^2)
A_F	Cross-sectional area of coolant (cm^2)
c_p	Specific heat (cal/gm-°C)
E	Internal energy per unit mass (cal/gm)
f	Friction factor
g	Acceleration of gravity (cm/sec^2)
G	Mass flow rate (gm/cm^2-sec)
H	Enthalpy per unit mass (cal/gm)
k	Thermal conductivity (cal/sec-cm-°C)
K	Coefficient in the friction factor relation
ℓ	Exponent in the viscosity-temperature relation
L	Core height (cm)
L'	Height of core plus stack region above it
L_{eq}	Equivalent length of the external piping
n	Exponent in the friction factor relation
p	Pressure (psia)
q_w	Surface heat flux (cal/cm^2-sec)
Q	Heat generation rate per unit volume at core midplane (cal/cm^3-sec)
r_H	Hydraulic radius A_F/P_w where P_w is the wetted perimeter (cm)
r_H'	Heated hydraulic radius A_F/P_H where P_H is the heated perimeter (cm)
R	Ratio of L' to L
t	Time (sec)
T	Temperature, absolute unless stated otherwise (°K)
u	Velocity of coolant (cm/sec)
x	Distance from core inlet (cm)

Dimensionless Numbers

Nu Nusselt Number, $4\, r_H\, h/k$

P Dimensionless Pressure, $p/\rho_1 gL$

Pr Prandtl number, $\mu c_p/k$

$\tilde{Q}$ Dimensionless midplane heat generation rate, $\left(\frac{4 r_H r'_H}{k_1 T_1 (A_F/A_f)}\right) Q$

Re Reynolds number, $4\, r_H\, G/\mu$

C Dimensionless constant, $16\, r_H^2\, \rho_1^2\, g\, L/\mu_1^2$

Greek Letters

δ Ratio of L_{eq} to L

ξ Dimensionless length measured from core entrance, x/L

θ Dimensionless temperature, T/T_1

μ Viscosity (poise)

ρ Density (gm/cm^3)

τ Dimensionless time, $\left(\frac{k_1 (A_F/A_f)}{4\, r_H r'_H\, (\rho c_p)_f}\right) t$

Subscripts

f Fuel

1 Inlet to core

REFERENCES

1. "Shippingport Hazards Summary Report", WAPD-SC-541, Atomic Power Laboratory (1957).

2. "Technical Inofrmation and Final Hazards Summary Report - Yankee", TID-6318, Yankee Atomic Electric Company (1960).

3. "Final Hazards Summary Report - Boiling Nuclear Superheater Power Station", PRWRA-GNEC-5, General Nuclear Engineering Corporation (1962).

4. "Final Hazards Summary Report for the Big Rock Point Plant", NP-11153, Consumers Power Company (1961).

5. ALEXIS W. LEMMON, JR., et al., "Core Temperature Excursions Following a Piping Failure in the Plutonium Recycle Test Reactor", BMI-1356, Battelle Memorial Institute (1959).

6. "Nuclear Merchant Ship Reactor Safeguards Report", BAW-1164, Babcock and Wilcox Company - Atomic Energy Division (1963).

7. S. E. JENSEN, et al., "Status Report, LOFT Loss of Coolant Thermal Transient Analysis", PTR-676, Phillips Petroleum Company (1964).

8. D. R. OLANDER, et al., "Safety Analysis for the U.C. Berkeley Research Reactor", University of California (1964).

9. K. SHURE, "Fission Product Decay Energy - Bettis Technical Review", WAPD-BT-24, Bettis Atomic Power Laboratory (1961).

10. R. P. OMBERG, "Effect of Natural Convection Upon the Temperature Transient Following a Loss-of-Coolant Accident in a Nuclear Power Reactor", (M.S. Thesis) UCRL-16394, Lawrence Radiation Laboratory (1965).

11. E. R. G. ECKERT and T. F. IRVINE, JR., "Incompressible Friction Factor, Transition and Hydrodynamic Entrance-Length Studies of

Ducts with Triangular and Rectangular Cross Sections", Fifth Mid-Western Conference on Fluid Mechanics, University of Michigan Press (1957).

12. E. R. G. ECKERT and T. F. IRVINE, JR., "Pressure Drop and Heat Transfer in a Duct with Triangular Cross Section", Trans. ASME, 82, 126 (1960).

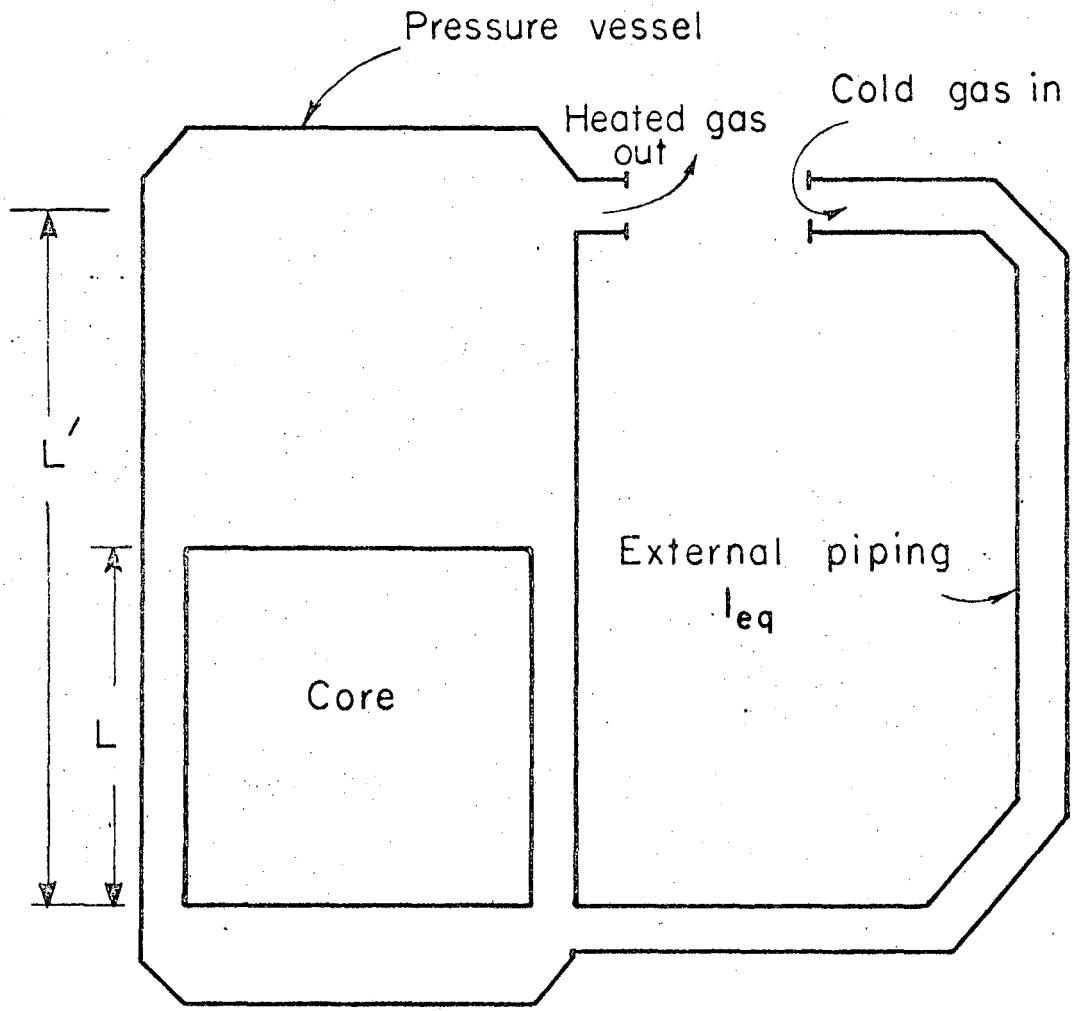

MU-36724

Fig. 1 Nuclear reactor configuration to which the conservation equations were applied.

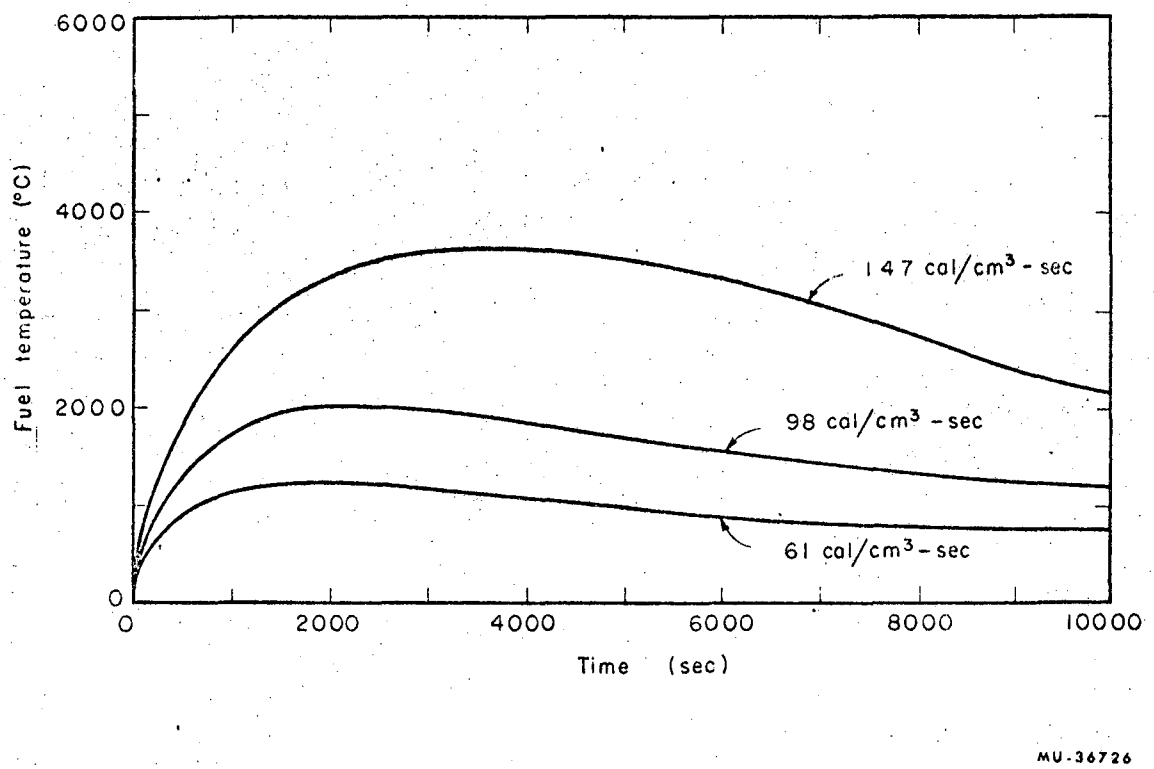

Fig. 2 Spatial maximum fuel temperature during the natural convection steam cooling temperature transient.

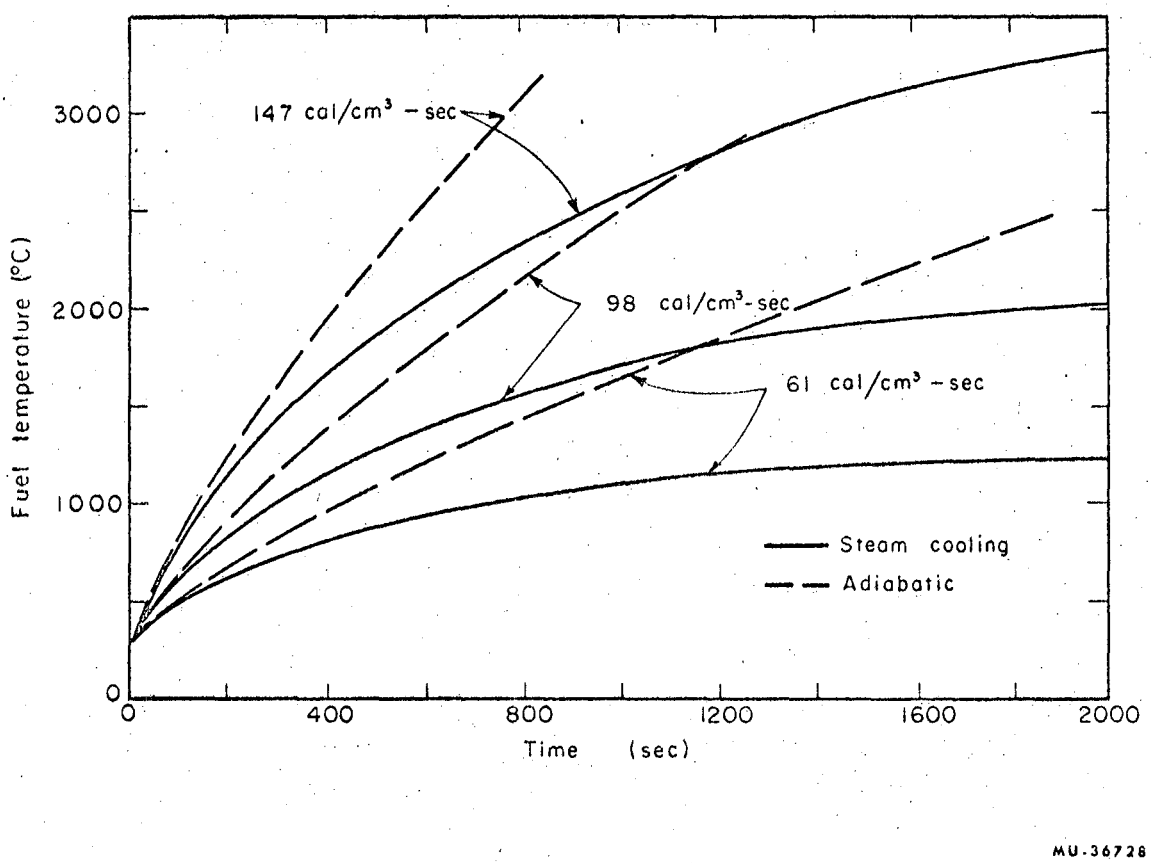

Fig. 3 Comparison of natural convection steam cooling and adiabatic temperature transients; the fuel temperature is the spatial maximum.

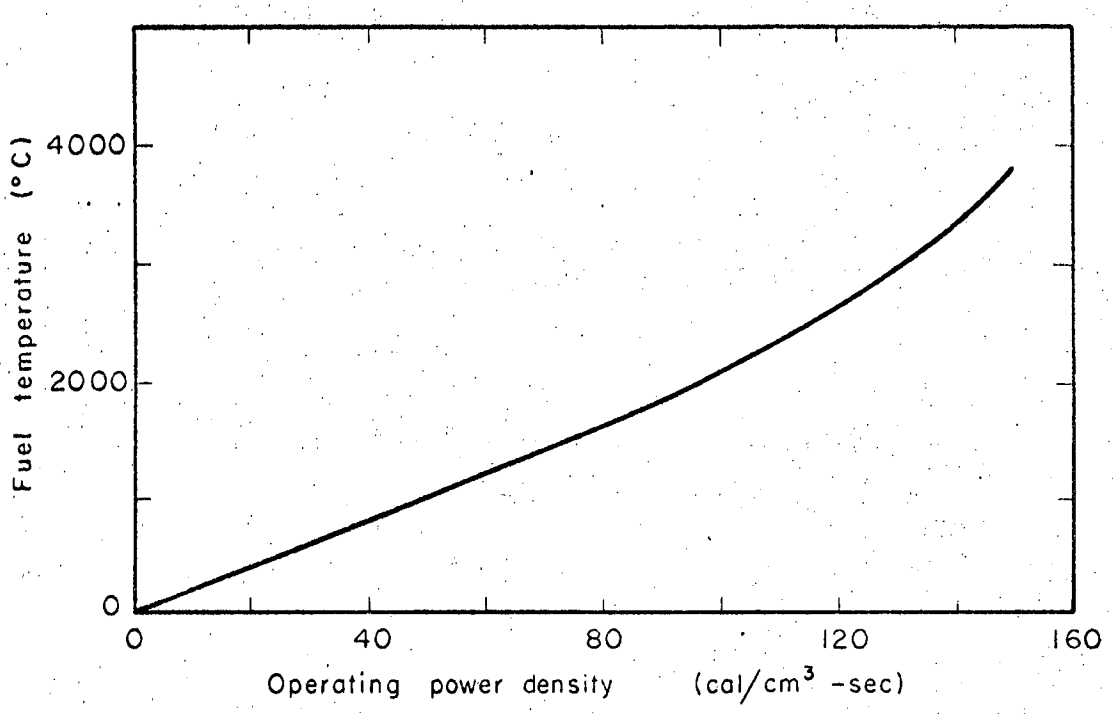

Fig. 4 Maximum fuel temperature (spatial and temporal maximum) during the transient vs power density.

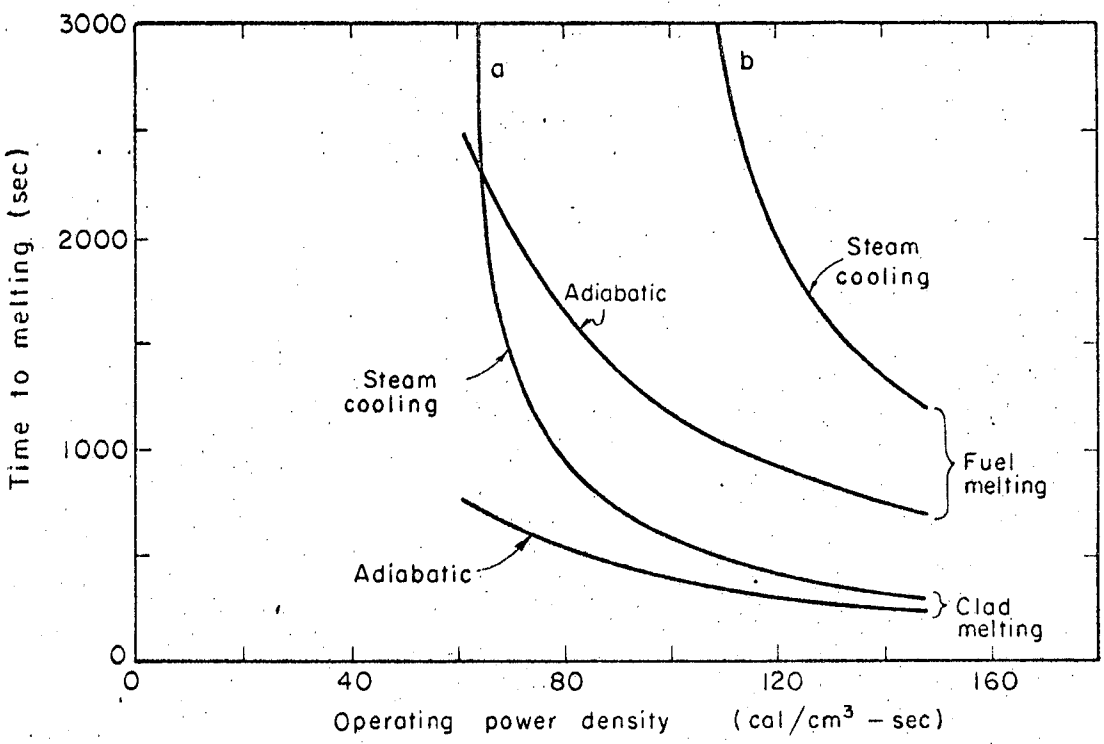

Fig. 5 Time to fuel and clad melting vs operating power density. Curve a melting point not attained at 61 cal/cm^3-sec. Curve b melting point not attained at 98 cal/cm^3-sec.

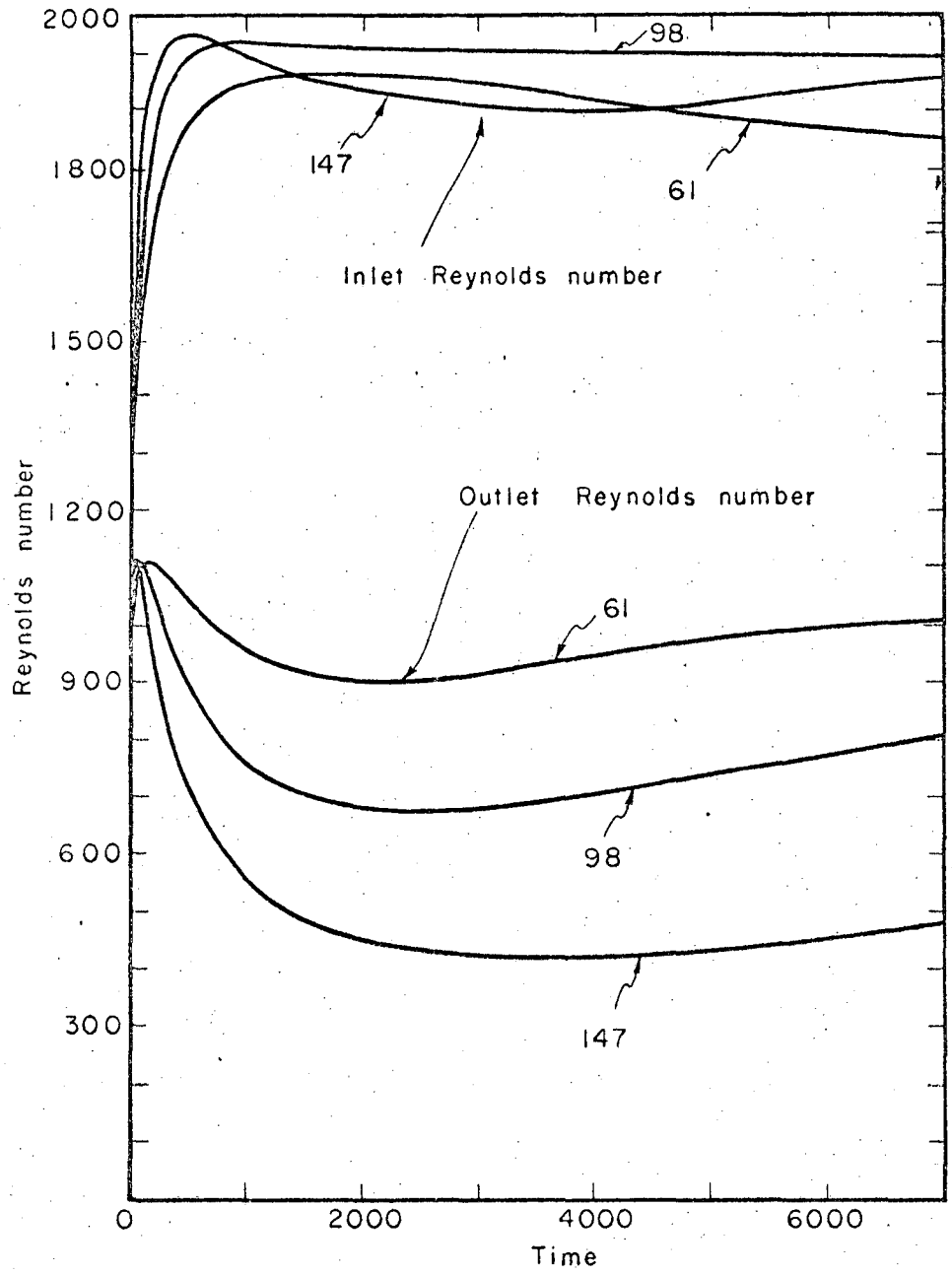

Fig. 6 Reynolds number at core inlet and outlet during transient.

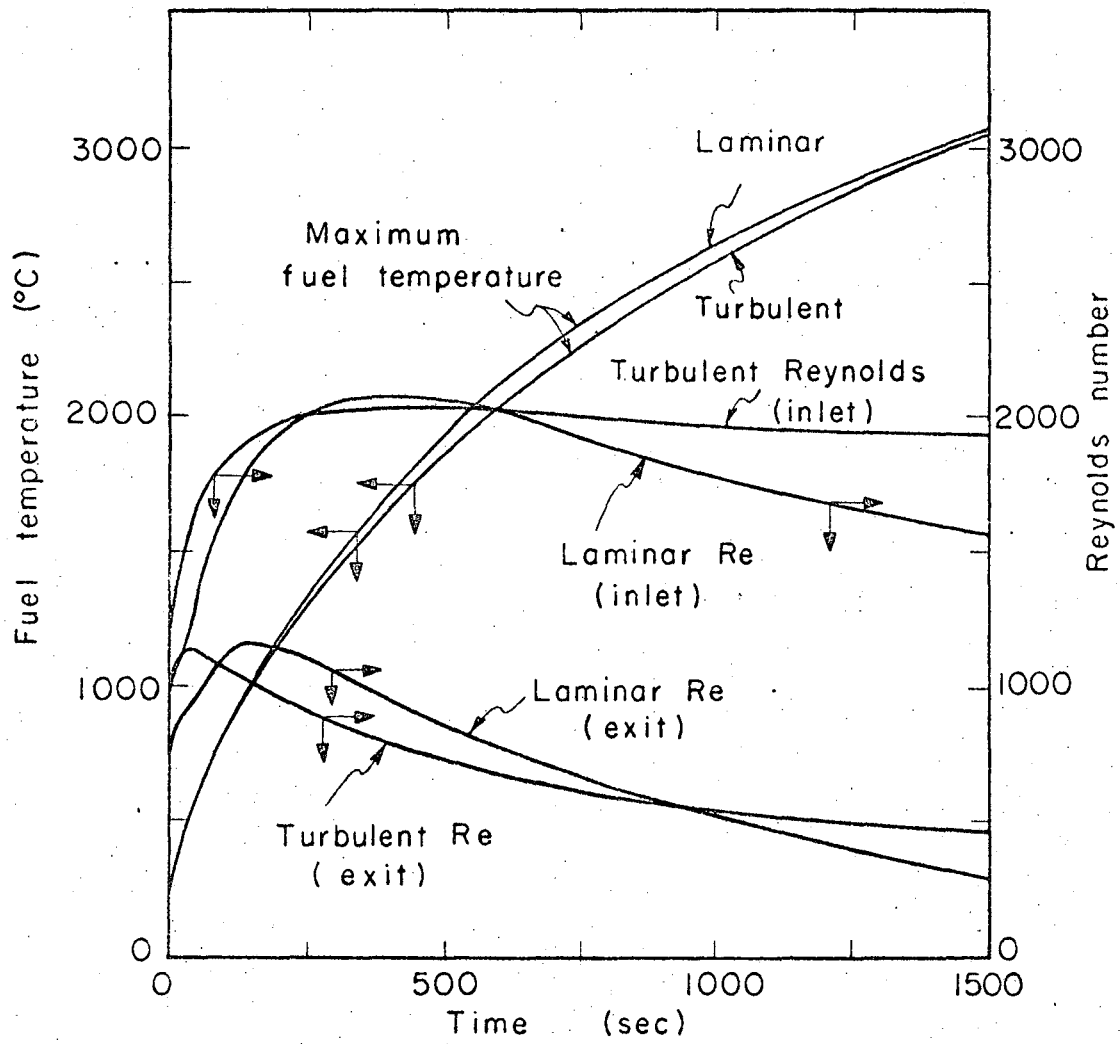

Fig. 7 Comparison of spatial maximum fuel temperatures and Reynolds numbers for steam cooling by laminar and trubulent flows at an operating power density of 147 cal/cm^3-sec.

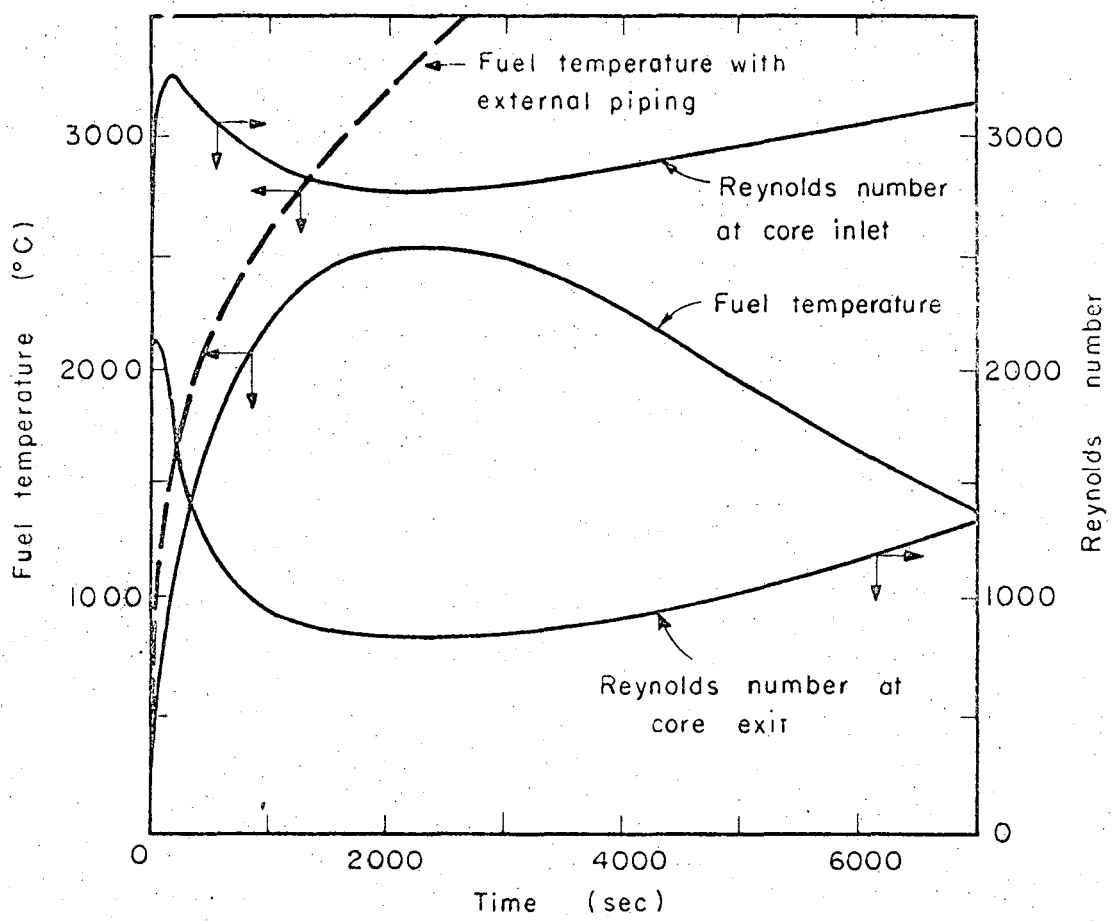

Fig. 8 Spatial maximum fuel temperature for the case of no external piping for an operating power density of 147 cal/cm^3-sec.